Effects of synthesis on electrochemical, structural and physical properties of solution phases of Li_2MnO_3–$LiNi_{1-x}Co_xO_2$

P.S. Whitfield, S. Niketic, I.J. Davidson [*]

Institute for Chemical Process and Environmental Technology, National Research Council Canada,
1200 Montreal Road, Ottawa, Ont., Canada K1A 0R6

Abstract

A study of the effect of synthesis techniques and conditions on the electrochemical, structural and physical properties of solution phases of Li_2MnO_3 and $LiNi_{1-x}Co_xO_2$ is reported. In this system, the formal oxidation state of the manganese is +4, while that of the nickel and cobalt is +3. These materials were produced from a variety of precursors and chelating agents. Modifications in the synthesis were found to affect the microstructure of the products and their electrochemical performance. It is demonstrated that, with good compositional and microstructural control, solution phases of Li_2MnO_3 and $LiNi_{1-x}Co_xO_2$ can have stable discharge capacities as high as $240\,mAh\,g^{-1}$. Furthermore, it has been found that a solution phase of Li_2MnO_3 and $LiNi_{1-x}Co_xO_2$, having no nickel content, $Li_{1.2}Mn_{0.4}Co_{0.4}O_2$, can produce very high discharge capacities ($\sim235\,mAh\,g^{-1}$) when charged to voltages greater than 4.3 V, despite an apparent theoretical capacity of only $125\,mAh\,g^{-1}$.
Crown Copyright © 2005 Published by Elsevier B.V. All rights reserved.

Keywords: Li_2MnO_3; Chelating agents; Electrochemical

1. Introduction

Solid solutions of Li_2MnO_3 and $LiMn_{0.5}Ni_{0.5}O_2$ [1–3] have received much attention recently as potential high capacity cathodes for lithium ion cells. These materials were found to exhibit anomalously high reversible capacities after charging to voltages greater than 4.3 V [1–4]. The addition of $LiCoO_2$ to solutions of Li_2MnO_3 and $LiMn_{0.5}Ni_{0.5}O_2$ was found to reduce the cell impedance [4]. More recently, it was showed that similar results can be obtained with solid solutions of Li_2MnO_3–$LiCoO_2$ [5] and that the Ni^{2+}–Ni^{4+} redox couple is not a requirement. Further performance enhancements were found for more complex solution phases of Li_2MnO_3–$LiNi_{1-x}Co_xO_2$ [5]. These materials contain Ni in the formal oxidation state of +3 rather than +2 as in the previous reports of anomalously high capacity materials. The discharge capacities obtained, as high as $240\,mAh\,g^{-1}$, were much greater than expected for 1:1 solid

solutions of Li_2MnO_3–$LiNi_{1-x}Co_xO_2$. However, even for Li_2MnO_3 it has been shown that charging to voltages greater than 4.3–4.4 V induces an unexpected reversible capacity [6].

As a general trend, developments in lithium battery cathode materials have resulted in the requirement to synthesize increasingly complex materials. The production of single-phase ternary, quaternary and even more complex systems is a major challenge for conventional solid-state synthesis. Increasingly, solution-based techniques such as sol–gel and co-precipitation are being applied to ensure adequate mixing of ions on a molecular level. This paper examines an alternative sucrose-based, Pechini-like method that has proven effective in producing single-phase complex oxides. The sucrose method was originally developed to produce nanoparticulate oxides, but is attractive in that it combines aspects of chelation, dispersion and combustion methods in a simple, hotplate-based technique. The technique has been demonstrated to be flexible and to allow for the synthesis of very complex, five cation compositions as single-phase materials [5].

* Corresponding author. Tel.: +1 613 990 0347; fax: +1 613 991 2384.
E-mail address: isobel.davidson@nrc.ca (I.J. Davidson).

2. Experimental

The synthetic technique used was a slight variation on that described for the production of nanocrystalline oxides [7,8]. Metal ions were added in the form of nitrates, water-soluble oxalate salts, acetates or a mixture of lithium formate + transition metal (TM) acetates in the required stoichiometries. Sucrose was added in a 4:1 molar ratio, yielding a chelate:cation ratio of 8:1 after the hydrolysis of sucrose to saccaric acid. An alternative chelating agent, DL-malic acid was also studied, at a molar ratio of 8:1 versus cations. After dissolution of the solids in de-ionized water, concentrated nitric acid was added until the pH of the solution was below 1. The solution was then heated on a hot-plate to evaporate the water. Once the solution started to become viscous, the heat was increased to decompose the salts, and eventually, char the mixture. This process produces a lot of gas and, with sucrose, the viscous mixture foams up considerably. However, very little foaming was observed when DL-malic acid was used as the chelating agent. Heating was continued until the char dried out and eventually combusted. Combustion is slow in this process as opposed to the rapid process that occurs with glycine, for example. Once combustion finished, the ashes were collected and fired in flowing air at temperatures ranging from 800 to 900 °C for 6 h.

Characterization by powder X-ray diffraction was carried out a Bruker D8 diffractometer equipped with double Göbel mirror, parallel-beam optics. Samples were mounted on zero background holders and analysed using Cu Kα radiation between 10° and 100° in 2θ. Unit cell parameters and size information were obtained by full-pattern fitting using TOPAS V2.1 software [9]. High resolution scanning and transmission electron microscope images were obtained using a Hitachi S4800 instrument on uncoated samples.

Electrochemical testing was carried out in coin cells (size 2325) constructed in an argon-filled glove box. The cathodes were prepared by casting slurries containing 80 wt% active material, 14 wt% carbon and 6 wt% binder in a fugitive solvent, onto aluminium foil. The individual electrodes, of 12.5 mm diameter, were pressed under a pressure of 0.5 tonnes. The cells were completed with lithium metal anodes, polypropylene separators (Celgard) and 70 μl of 1 M $LiPF_6$ in 1:1 EC/DMC electrolyte solution. Galvanostatic cycling was carried out at a rate of 10 mA g^{-1} between 2.0 and 4.6 V.

3. Results and discussion

All of the compositions were confirmed to be single-phase by X-ray diffraction, with patterns consistent with a Li_2MnO_3-type C2/m monoclinic unit cell. The smooth evolution of unit cell parameters with composition along the phase diagram tie line was consistent with solid-solution behaviour [5].

Table 1
Refined pseudo-hexagonal cell parameters and size (LVol-IB) information for the different materials obtained by full pattern fitting

Preparation	a (Å)	c (Å)	Size (LVol-IB) (nm)
$Li_{1.2}Mn_{0.4}Ni_{0.3}Co_{0.1}O_2$, 800 °C			
Li formate + acetates (sucrose)	2.8532(1)	14.2101(1)	92(5)
Acetates (sucrose)	2.8537(1)	14.2112(10)	74(4)
Oxalates (sucrose)	2.8549(2)	14.1923(17)	39(2)
Nitrates (DL-malic acid)	2.8509(1)	14.2030(10)	100(5)
Nitrates (sucrose)	2.8519(1)	14.2077(8)	66(4)
$Li_{1.2}Mn_{0.4}Ni_{0.2}Co_{0.2}O_2$, 800 °C			
Nitrates (sucrose)	2.8462(1)	14.1912(8)	66(7)
$Li_{1.2}Mn_{0.4}Ni_{0.1}Co_{0.3}O_2$, 900 °C			
Nitrates (sucrose)	2.8386(1)	14.1893(5)	164(16)
$Li_{1.2}Mn_{0.4}Co_{0.4}O_2$, 900 °C			
Nitrates (sucrose)	2.8294(1)	14.1662(7)	134(17)

For comparison with prior studies on solution phases of Li_2MnO_3 and $LiMn_{0.5}Ni_{0.5}O_2$, lattice parameters were refined using the related pseudo-hexagonal *R-3m*-type unit cell. The lattice parameters, provided in Table 1, varied predictably with Ni/Co ratio but showed little change with variations in precursors or chelating agents. There was some variation, however, in the size parameter, volume-weighted column length from integral breadth (LVol-IB) [10], with composition, and with variations in precursors and chelating agents. Such variations can be due to differences in the dispersion and combustion stages of the process that result from variability in foaming and quantities of available fuel. Furthermore, the requirement for human intervention to control the combustion may have contributed to the variability.

The discharge capacities, for the first 50 cycles, for cells containing 1:1 solution phases of Li_2MnO_3 and $LiNi_{1-x}Co_xO_2$ are shown in Fig. 1. Electrochemical per-
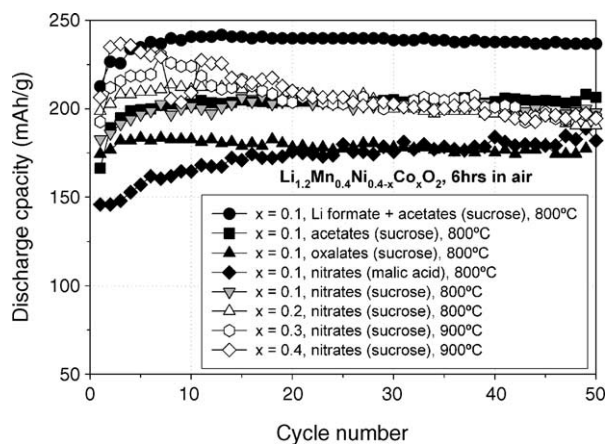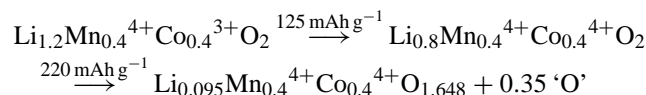

Fig. 1. Capacity vs. cycle number for $Li_{1.2}Mn_{0.4}Ni_{0.4-x}Co_xO_2$ with $x = 0.1$ for Li formate + TM acetates, acetates, oxalates and nitrate precursors using sucrose chelating agent, and nitrates with DL-malic acid as a chelating agent. Also shown are discharge capacities for the series $x = 0.1$–0.4 produced using nitrates with sucrose chelating agent.

formance was evaluated as a function of Ni:Co ratio, using nitrate salts and sucrose, and as a function of the choice of precursors and chelating agents at a fixed composition, $Li_{1.2}Mn_{0.4}Ni_{0.3}Co_{0.1}O_2$. $Li_{1.2}Mn_{0.4}Ni_{0.3}Co_{0.1}O_2$ was prepared at 800 °C, but compositions with greater cobalt content required a higher firing temperature (900 °C) to obtain stable electrochemical performance. The variation in discharge capacities as a function of Ni:Co ratio is surprisingly small. In particular, $Li_{1.2}Mn_{0.4}Co_{0.4}O_2$ (at $x = 0.4$) produced discharge capacities of as high as 235 mAh g^{-1}, despite the complete lack of nickel in the system and having a "theoretical" capacity of only 125 mAh g^{-1}. Indeed, in a previous study on solid solutions of Li_2MnO_3 and $LiCoO_2$ in which cells were cycled between 3.0 and 4.3 V, the capacities decreased with increasing Mn content [11]. Variations in precursors and chelating agents were found to affect the capacities and capacity retention of $Li_{1.2}Mn_{0.4}Ni_{0.3}Co_{0.1}O_2$. The best performing material prepared from Li-formate and acetate salts of the transition metals yielded an ultimate discharge capacity of approximately 240 mAh g^{-1}, with very good capacity retention.

Charge–discharge voltage profiles are shown in Fig. 2 for 1:1 solution phases of Li_2MnO_3 and $LiNi_{1-x}Co_xO_2$ prepared from nitrate salts and sucrose for a range of Ni:Co ratios, and for $Li_{1.2}Mn_{0.4}Ni_{0.3}Co_{0.1}O_2$ prepared from nitrate salts and DL-malic acid and from Li-formate and TM acetate salts with sucrose. All materials in these series exhibited the irreversible voltage plateau at 4.4–4.5 V, characteristic of anomalous capacities, on the first cycle. After completion of this formation step, voltage profiles more characteristic of a layered α-NaNiO₂-type structure were established.

In previous studies on solid solutions of Li_2MnO_3 and $LiNi_{0.5}Mn_{0.5}O_2$ [2], the formation step on first charge has been attributed to oxygen loss through simultaneous extraction of Li and O from the materials. The similarities in the voltage curves in Fig. 2 with those for solutions of Li_2MnO_3 and $LiNi_{0.5}Mn_{0.5}O_2$ suggest that the same process is occurring. Taper charging of $Li_{1.2}Mn_{0.4}Co_{0.4}O_2$ produced a first charge capacity of 345 mAh g^{-1}. Attributing the excess capacity on the first charge to simultaneous loss of Li and O, this would be consistent with the following:

$$Li_{1.2}Mn_{0.4}{}^{4+}Co_{0.4}{}^{3+}O_2 \xrightarrow{125\,\text{mAh g}^{-1}} Li_{0.8}Mn_{0.4}{}^{4+}Co_{0.4}{}^{4+}O_2$$
$$\xrightarrow{220\,\text{mAh g}^{-1}} Li_{0.095}Mn_{0.4}{}^{4+}Co_{0.4}{}^{4+}O_{1.648} + 0.35\,\text{'O'}$$

$Li_{0.095}Mn_{0.4}Co_{0.4}O_{1.648}$ would conventionally be described as $Li_{0.115}Mn_{0.486}Co_{0.486}O_2$. Full re-lithiation to $Li_{1.028}Mn_{0.486}Co_{0.486}O_2$ on discharge would require 234 mAh g^{-1} of the original $Li_{1.2}Mn_{0.4}Co_{0.4}O_2$. Consequently, the reversible capacity observed, 235 mAh g^{-1}, indicates that the material formed in situ after charging to high voltages can be almost fully ($\sim$90%) delithiated in a reversible manner under favourable conditions.

The effects of variations in the precursors and chelating agents on a fixed composition, $Li_{1.2}Mn_{0.4}Ni_{0.3}Co_{0.1}O_2$, can be seen in Fig. 2d–f. The material produced from Li formate + TM acetates with sucrose (Fig. 2f) showed the largest reversible capacity and a low internal resistance as is evident at the end of charge. Similar behaviour was found using nitrates with sucrose (Fig. 2e), but the reversible capacities were lower. Fig. 2e shows the performance of $Li_{1.2}Mn_{0.4}Ni_{0.3}Co_{0.1}O_2$ produced using nitrates, but with DL-malic acid instead of sucrose as the chelating agent. These cells exhibited significant cell polarisation, which decreased the reversible capacity and prolonged the number of cycles needed to complete the formation step (shown in Fig. 1).
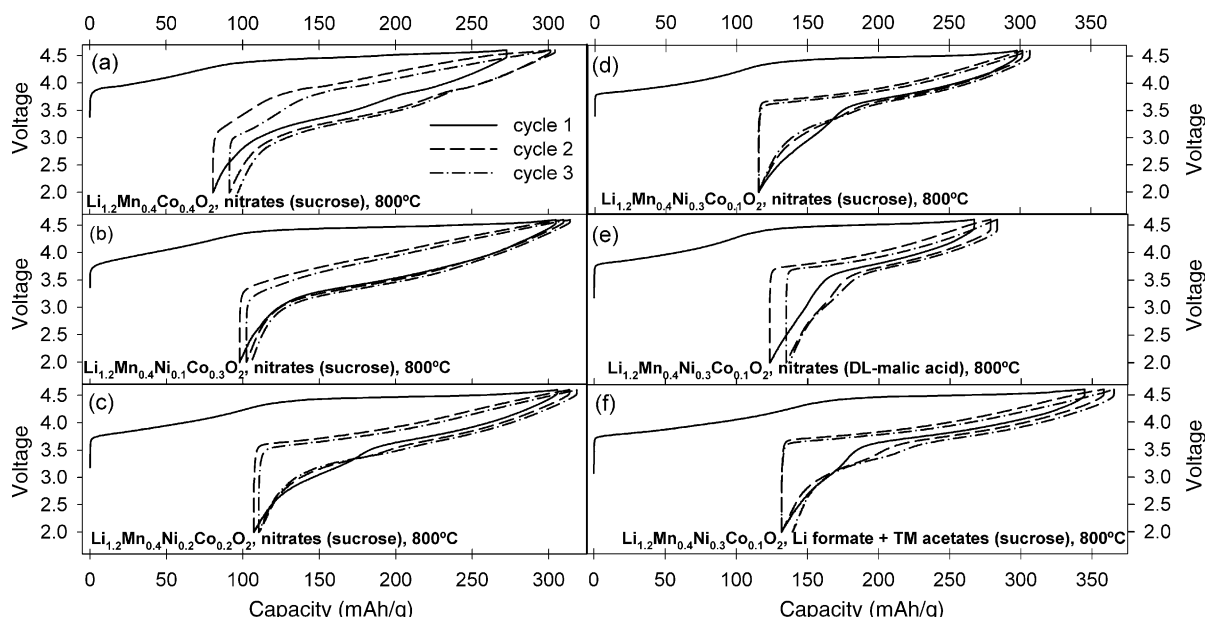

Fig. 2. Voltage curves for $Li_{1.2}Mn_{0.4}Ni_{0.4-x}Co_xO_2$ with $x = 0.4$–0.1 produced using nitrates with sucrose chelating agent, and for $x = 0.1$ using Li formate + TM acetates with sucrose, and nitrates with DL-malic acid as chelating agents, respectively.
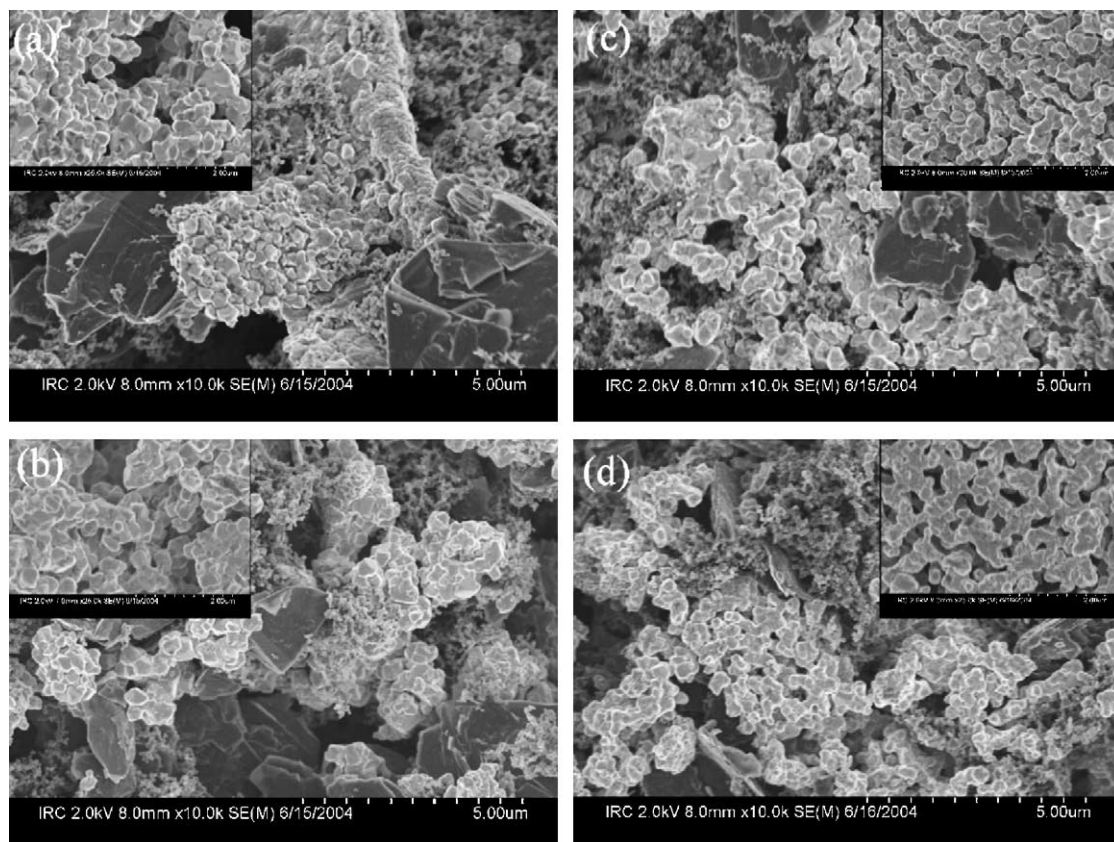
Fig. 3. Scanning electron microscopy (SEM) images of electrode surfaces for $Li_{1.2}Mn_{0.4}Ni_{0.3}Co_{0.1}O_2$ prepared from (a) nitrates with sucrose, (b) nitrates with DL-malic acid, (c) Li formate + TM acetates with sucrose and (d) acetates with sucrose, with SEMs of the corresponding $Li_{1.2}Mn_{0.4}Ni_{0.3}Co_{0.1}O_2$ powders inset.

The variation in electrochemical performance of materials with the same composition and structural features suggested that microstructural characteristics were affecting the cell performance. Consequently, a SEM study of the $Li_{1.2}Mn_{0.4}Ni_{0.4-x}Co_xO_2$ powders and the cast electrodes was undertaken. Fig. 3 shows the SEM micrographs of the casts with an inset of the $Li_{1.2}Mn_{0.4}Ni_{0.4-x}Co_xO_2$ powders at higher magnification. Fig. 3a and b show materials produced using nitrates with sucrose and DL-malic acid, respectively. The material produced using DL-malic acid has many fused, large agglomerates, while the material produced using sucrose produced more loosely bound, if still large agglomerates with intra-granular porosity. The cast produced from these materials is also different. The cast produced with sucrose contains large, but porous grains together with some unusual, filament-like structures. The cast produced using DL-malic acid contains smaller, but dense, sintered spherical particles. This morphology affected the kinetics of the formation process and led to the slow rise in discharge capacities. Fig. 3c and d show the materials produced with sucrose using Li formate + TM acetates, and only acetates, respectively. In both cases, an open, porous microstructure is observed, although Fig. 3d shows a more tightly bound 3D network. The increased porosity of these materials could in part be due to the additional carbonaceous fuel supplied by the organic precursors. Differences

in binding of the 3D network could be due to the speed and temperature of combustion. This in turn would be related to the porosity of the carbonaceous foam before combustion. The foaming process could be tuned by the use of cross-linking agents to increase the density of the polymerised matrix.

4. Conclusions

This study has shown the versatility of a modified Pechini method for the preparation of complex solid solutions with controlled microstructure. Through judicious selection of chelating agents and precursors, it was possible to tune the microstructure of solid solutions of Li_2MnO_3–$LiNi_{1-x}Co_xO_2$ for better dispersion in the electrodes. The optimal microstructure has a loosely bound network structure of small, uniform particles. Such a structure is friable, and is easily and uniformly dispersed throughout an electrode during processing.

In conclusion, nanoscale materials in the series Li_2MnO_3–$LiNi_{1-x}Co_xO_2$ can yield very high discharge capacities ($\sim$240 mAh g^{-1}), but require careful microstructural control to produce electrodes with good electrochemical performance. The presence of Ni^{2+} is not required to produce the anomalously high capacities that have been widely reported.

Indeed, similar behaviour can be produced in materials containing no nickel at all.

Acknowledgement

References

[1] S.H. Kang, K. Amine, J. Power Sources 124 (2003) 533–537.
[2] Z. Lu, J.R. Dahn, J. Electrochem. Soc. 149 (2002) A815–A822.
[3] S.-S. Shin, Y.-K. Sun, K. Amine, J. Power Sources 112 (2002) 634–638.
[4] J.-H. Kim, C.W. Park, Y.-K. Sun, Solid State Ionics 164 (2003) 43–49.
[5] P.S. Whitfield, S. Argue, I.J. Davidson, Systematic investigation of $Li_{1+\delta}(Mn,M',M'')_{1-\delta}O_2$ ($\delta \Rightarrow 0$; M' and $M'' =$ transition metals). The Li_2MnO_3–$LiNi_{1-x}Co_xO_2$ solid solution series, in: Second Lithium Battery Discussion, Arcachon, France, 15–19 September, 2003 (Abstract No. 59).
[6] A.D. Robertson, P.G. Bruce, Chem. Commun. (2002) 2790–2791.
[7] R.S. Das, A. Bandyopadhyay, S. Bose, J. Am. Ceram. Soc. 84 (2001) 2421–2423.
[8] L.D. Mitchell, P.S. Whitfield, J. Margeson, J.J. Beaudoin, J. Mater. Sci. Lett. 21 (2002) 1773–1775.
[9] Bruker AXS, TOPAS V2.1, General profile and structure analysis software for powder diffraction data, User Manual, Bruker AXS, Karlsruhe, Germany, 2003.
[10] D. Balzar, S. Popoviæ, J. Appl. Crystallogr. 29 (1996) 16–23.
[11] K. Numata, C. Sakaki, S. Yamanaka, Solid State Ionics 117 (1999) 257–263.